

## GEOMETRIC EFFECTS IN AVALANCHE MODELS OF SOLAR FLARES: IMPLICATIONS FOR CORONAL HEATING

S. W. McINTOSH

European Space Agency, Space Science Department, NASA Goddard Space Flight Center, Mailcode 682.3, Greenbelt, MD 20771; scott@esa.nascom.nasa.gov

AND

P. CHARBONNEAU

High Altitude Observatory, National Center for Atmospheric Research, P.O. Box 3000, Boulder, CO 80307; paulchar@hao.ucar.edu

Received 2001 October 12; accepted 2001 November 15; published 2001 December 7

### ABSTRACT

Observational inferences of the power-law frequency distribution of energy release by solar flares, and in particular its logarithmic slope  $\alpha_E$ , depend critically on the geometric relationship assumed to relate the observed emitting area  $A$  and the underlying emitting volume  $V$ . Recent results on the fractal nature of avalanches in self-organized critical models for solar flares indicate that this relationship is a power law  $V \propto A^\gamma$  with index  $\gamma = 1.41(\pm 0.04)$ . We show that when proper account is made for the fractal geometry of the flaring volume, hitherto discrepant observational inferences of  $\alpha_E$  are brought in much closer agreement. The resulting values of  $\alpha_E$  lie tantalizingly close, but still below the critical value  $\alpha_E = 2.0$ , beyond which Parker’s conjecture of coronal heating by nanoflares is tenable.

*Subject headings:* Sun: flares — Sun: magnetic fields — Sun: UV radiation — Sun: X-rays, gamma rays

### 1. INTRODUCTION

The last decade has witnessed an unprecedented increase in the body of observational data on solar flares, through a sequence of spaceborne instruments with ever-increasing spatial and temporal resolution. These data allow us, in principle, to quantitatively address Parker’s conjecture of coronal heating by nanoflares (e.g., Parker 1988). The crux of the matter is the form of the frequency distribution  $f(E)$  of energy release by flares [such that  $f(E)dE$  is the fraction per unit time of flares releasing energy in the range  $E$  to  $E + dE$ ]. The related frequency distribution for raw peak flux (counts  $\text{s}^{-1}$ , say) is known to be a well-defined declining power law in peak flux (e.g., Dennis 1985), suggesting that  $f(E)$  is itself a declining power law in flare energy  $E$ :

$$f(E) = f_0 E^{-\alpha_E}, \quad \alpha_E > 0. \quad (1)$$

From the coronal heating point of view, the key lies in the numerical value of  $\alpha_E$ : it is readily shown that the smaller flares dominate energy input to the corona provided  $\alpha_E > 2$ , which then becomes a sine qua non condition for Parker’s conjecture.

Because of their characteristic spatial and temporal self-similarity, avalanche models for solar flares provide a natural explanation for the observed power laws in flare parameters (see Lu & Hamilton 1991; Lu et al. 1993; and Charbonneau et al. 2001 for a pedagogical introduction and a recent review of these models). The basic credo is that a flare is the collective manifestation of energy released by an avalanche of small-scale reconnection events, cascading through coronal magnetic field structures mechanically stressed by stochastic motions of their photospheric footpoints. In fact, Parker’s nanoflare picture includes all the ingredients deemed necessary to lead to *self-organized criticality* (SOC; Bak, Tang, & Wiesenfeld 1987; Jensen 1998): a slowly driven (photospheric footpoint motions) open system (magnetic structure embedded in the solar corona) subject to a self-stabilizing local threshold instability (magnetic reconnection) leading to localized transport and readjustment of the physical quantity subject to instability (Lu 1995; Charbonneau et al. 2001). Such systems are well known to release

energy intermittently, in the form of episodic avalanches with power-law size distribution. In the context of such models, there is no fundamental difference between a large “classical” X-ray flare and small transient brightening such as observed in the EUV; the latter is just a much smaller avalanche of reconnection events than the former.

The avalanche model for solar flares has done quite well in reproducing the form and logarithmic slope of the observed frequency distribution  $f(P)$  of peak flux  $P$  (see Lu & Hamilton 1991). For the net energy release,  $E$ , the comparison is less favorable, with observed inferences yielding a wide range of  $\alpha_E$ , with most values, moreover, significantly larger than in the model (see Charbonneau et al. 2001, and references therein).

It is not yet clear how severe this discrepancy is, given that the inferred  $f(E)$  is far more model dependent than the corresponding distribution for peak flux. The quantity actually observed, the spectral intensity of line  $i$ ,  $I_i = P_i/(4\pi A)$  for spectral power  $P_i$  and projected emitting area  $A$ , can be written as

$$I_i = \int_{T_e} K_i(T_e) \xi(T_e) dT_e \text{ ergs cm}^{-2} \text{ sr}^{-1} \text{ s}^{-1}, \quad (2)$$

where  $\xi(T_e)$  is the differential emission measure in temperature (DEM),  $K_i(T_e)$  is the line/bandpass emissivity, and any dependence on the electron density  $n_e$  has been neglected (see Craig & Brown 1976; McIntosh 2000). Most often,  $K_i(T_e)$  is strongly peaked, so that the intensity can be assumed to be proportional to the value of  $\xi_i(T_e)$  in a narrow band ( $\pm 0.1$  dex) about the peak temperature of line formation  $T_e^*$ . In the limit  $K_i(T_e) \rightarrow \mathcal{K}_i \delta(T_e - T_e^*)$  [ $\delta(x - x_0)$  being the Dirac delta function], equation (2) can be expressed in terms of the integrated intensity flux  $f(= I_i/A) \approx \mathcal{K}_i \xi(T_e^*)/A$  (ergs  $\text{cm}^{-4} \text{ s}^{-1}$ ).

Following Brown et al. (1991), we assume  $\xi(T_e) = n_e^2 h$ , where  $h$  is the column depth, and obtain an estimate for the electron density (with filling factor of unity):  $n_e = [\xi(T_e^*)/h]^{1/2}$  (units:  $\text{cm}^{-3}$ ). This estimate allows us to calculate the net thermal energy release underlying the observed emis-

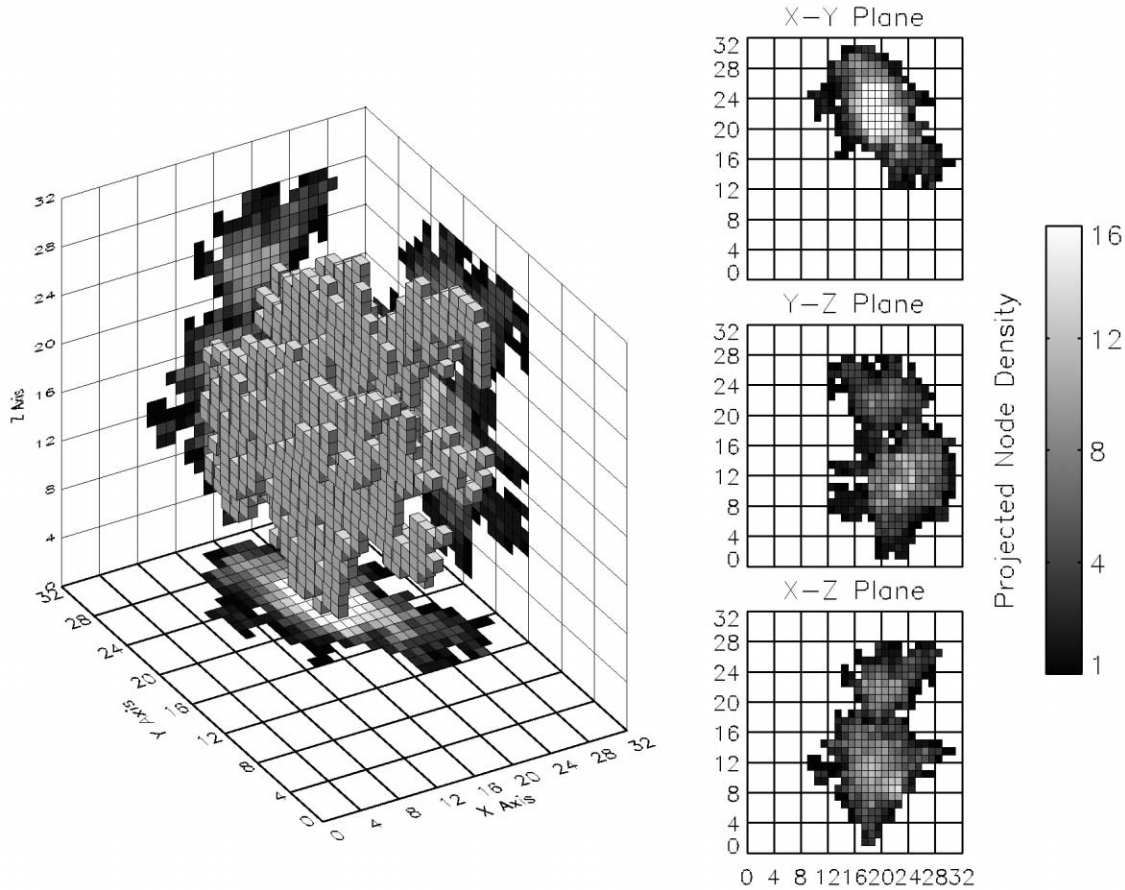


FIG. 1.—The three-dimensional structure of the time-integrated avalanche in a  $32^3$  lattice. Here 5145 lattice nodes, plotted as small cubic blocks, have gone unstable at least once over the duration of the avalanche. This cluster is the model's equivalent to the flaring volume  $V$  on the right-hand side of eq. (3). The right-hand side of the figure shows views of the projections of the time-integrated cluster on the three coordinate planes of the lattice. The gray scale in the projected planes indicates the number of avalanching nodes, or column depth, along the projection line of sight.

sion:

$$\mathcal{E}_{th} = 3n_e k_B T_e^* V \text{ ergs}, \quad (3)$$

where  $V$  is the volume of the emitting plasma. A common (and probably reasonable) assumption is that of constant pressure,  $\propto n_e T_e$ , within coronal structures (see, e.g., Raymond & Doyle 1981), so that the remaining dependency is on the flaring volume, which must then be related to the observed projected area via some geometric model. Such models include, for example, the loop model of Aschwanden et al. (2000), leading to  $V \propto A^{3/2}$  (with constant filling factor), or the so-called cylinder model, where it is assumed that the flaring volume is a column of height  $h$  extending below the projected area, yielding  $V \propto A$  for constant  $h$ , or  $V \propto A^{3/2}$  for the alternate common assumption  $h \propto \sqrt{A}$  (see, e.g., Parnell & Jupp 2000; Krucker & Benz 1998; Mitra-Kraev & Benz 2001).

## 2. THE FLARING VOLUME AS A FRACTAL OBJECT

We have performed a large series of simulation runs using what is essentially a scalar version of the Lu et al. (1993) three-dimensional avalanche model. Full details concerning the model and numerical implementation can be found in Charbonneau et al. (2001). McIntosh et al. (2001) have performed a detailed analysis of the geometric properties of avalanches in that model and have presented results pertaining to the fractal dimensions and frequency distributions of av-

alanche parameters for model runs carried out on two- and three-dimensional lattices.

Of particular interest in the present context is the form of the relationship existing between the avalanche *volume*  $V$ , defined as the total number of lattice nodes having gone unstable at least once in the course of the avalanche, and the *projected area*  $A$  of the avalanche, corresponding to the volume projected onto some arbitrary plane, which, for computational convenience and without any loss of generality, we take to be one of the three lattice coordinate planes. The area is thus the number of nodes in the two-dimensional projection plane for which at least one node along the corresponding perpendicular line of sight has gone unstable at least once in the course of the avalanche. Figure 1 illustrates a cluster of lattice nodes that have avalanched at least once in the course of a large avalanche and the three orthogonal projections thereof, shown on the right of the figure. The three-dimensional cluster is the model's equivalent to the emitting volume on the right-hand side of equation (3). Clearly, this geometrically complex object has an intricate structure that could hardly be guessed from any of its projected views.

A scatter plot of volume versus projected area (Fig. 2) reveals a power-law relationship of the form  $V \propto A^\gamma$ , with  $\gamma = 1.41(\pm 0.04)$ . Table 1 shows that the value of  $\gamma$  is stable as the lattice size is varied. Interestingly, this value corresponds to neither of the exponents for the two geometric models most often used in flare data analyses, namely,  $\gamma = 1$  for the cylinder model with constant column depth  $h$  and  $\gamma = 1.5$  for the loop

TABLE 1

POWER-LAW INDICES  $\gamma$  OF THE RELATIONSHIP BETWEEN AVALANCHE VOLUME AND PROJECTED AREA FOR THREE-DIMENSIONAL LATTICES OF VARIOUS LINEAR SIZE  $L$

$L$	$\gamma$
16 .....	$1.44 \pm 0.05$
24 .....	$1.41 \pm 0.04$
32 .....	$1.40 \pm 0.03$
48 .....	$1.42 \pm 0.04$
64 .....	$1.41 \pm 0.04$

model and cylinder model with  $h \propto \sqrt{A}$ . With the avalanche model taken at face value, this implies that extant observational analyses have either overestimated ( $\gamma = 1$ ) or underestimated ( $\gamma = 1.5$ ) the emitting volume of the smaller avalanches, as compared to that of the larger avalanches. The net effect is, as per equation (3), a steepening ( $\gamma = 1$ ) or flattening ( $\gamma = 1.5$ ) of the flare energy frequency distribution.

### 3. CORRECTING FOR GEOMETRIC EFFECTS

The task now at hand is simple. We must express the observationally inferred frequency distribution  $f(E)dE$  in terms of a new energy release variable  $E' [= s(E)E]$  corrected for geometric rescaling in terms of the fractal dimension of avalanches, through the term  $s(E)$ . Let  $\beta$  be the logarithmic slope of the (nonfractal)  $V$ - $A$  relationship used in observational analyses. In terms of projected areas, the correction factor  $s$  to the inferred emitting volume is evidently something like  $s(A) = A^\beta/A^\beta$ . With  $E \propto A^\beta$ , this yields

$$s(E) = E^{(\gamma-\beta)/\beta}. \quad (4)$$

The quantity  $f(E')dE'$  must now be expressed in terms of  $f(E)dE$ . With the latter given by equation (1), some straightforward algebra leads to

$$f(E')dE' = f(sE) \frac{dE'}{dE} dE \propto f_0 E^{-(\alpha_E + \Delta\alpha)} dE, \quad (5)$$

where the correction factor  $\Delta\alpha$  to the power-law index  $\alpha_E$  is given by

$$\Delta\alpha = \frac{(1 - \alpha_E)(\beta - \gamma)}{\beta}. \quad (6)$$

Table 2 lists a selection of  $\alpha_E$  values inferred by various recent observational analyses of UV/EUV data, together with the “corrected” values obtained by adding the  $\Delta\alpha$  as computed above. It is remarkable that previously widely discrepant inferences for  $\alpha_E$  are now brought in much better agreement when the fractal nature of the flaring volume is taken into consideration.<sup>1</sup>

### 4. DISCUSSION

Working within the framework of an avalanche model for solar flares, we have argued that the heated plasma responsible for the emission of observed short-wavelength radiation is distributed in a geometrically complex emitting volume. Cylinder models with constant  $h$  overestimate the emitting volume of

<sup>1</sup> Note that the  $\alpha_E$  value of Aschwanden et al. (2000) is obtained in a loop model characterized by a filling factor that scales with event size as a power law; this is why  $\beta = 1.44$  in their model, as opposed to 1.5 for a model with constant filling factor.

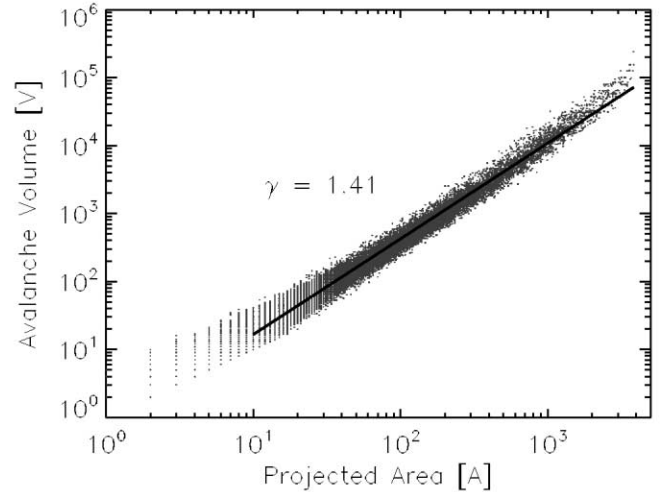


FIG. 2.—Scatter plot of 0.27 million time-integrated avalanche volumes  $V$  and projected areas  $A$  for a typical  $64^3$  lattice simulation. A power law with index  $\gamma = 1.41$  yields a good fit. Errors on the fit are estimated by running the model several times, each with a different random “seed” (see Charbonneau et al. 2001 for further details), to compute a Monte Carlo estimate of the power-law index, in this instance  $\gamma = 1.41 \pm 0.04$ .

smaller flares, as compared to large ones, and consequently produce markedly too steep a frequency distribution of energy release. The loop model of Aschwanden et al. (2000), or the cylinder model with  $h \propto \sqrt{A}$ , on the other hand, leads to a slight underestimate of the power-law index  $\alpha_E$  of this frequency distribution. Interestingly, using our model results to correct for these geometric effects brings hitherto discrepant results into much better agreement with one another. Although this interesting result should not be overinterpreted, it does demonstrate that geometric assumptions play a major role in the reconstruction of thermal energy release from short-wavelength observations of solar flares, and that some of the geometric models used thus far in observational analyses are quite possibly far removed from reality.

The possibility remains that different versions of the avalanche model could yield significantly different  $\gamma$  values and, thus, corrected  $\alpha_E$  indices numerically distinct from those listed in Table 2. We conjecture that all avalanche models characterized by local and isotropic instability criteria and redistribution rules (see Charbonneau et al. 2001 for more on these model ingredients) will have similar values of  $\gamma$ ; we base this conjecture on the relative robustness of the frequency distributions of avalanche parameters within the “local/isotropic” subset of possible avalanche models. This is clearly an issue that merits further investigation.

Most geometrically corrected values for  $\alpha_E$ , listed in Table 2 herein, lie tantalizingly close to, although still distinctly below, the transition value  $\alpha_E = 2.0$  above which Parker’s conjecture of coronal heating by nanoflare is tenable in principle (obviously, the global flaring rate parameter  $f_0$  in eq. [1] must also be high enough). Our geometric correction procedure has neglected any possible dependency of other physical quantities (electron density, temperature, etc.) on event size. Not surprisingly, introducing such dependencies can lead to further variations in the resulting  $\alpha_E$  and, under suitable numerical choices, can lead to  $\alpha_E > 2$  (see, e.g., Mitra-Kraev & Benz 2001, § 2).

As shown in McIntosh et al. (2001), distinct fractal dimensions and associated power-law relationships are obtained if

TABLE 2  
GEOMETRIC “CORRECTIONS” TO RECENT ANALYSES OF UV/EUV FLARE ENERGY RELEASE

Reference	Geometric Model	$\beta$	$\alpha_E$	$\alpha_E + \Delta\alpha$
Krucker & Benz 1998 .....	Cylinder, constant $h$	1.00	2.30–2.60	1.77–1.94
Parnell & Jupp 2000 .....	Cylinder, constant $h$	1.00	2.42	$1.84 \pm 0.04$
Parnell & Jupp 2000 .....	Cylinder, $h \propto \sqrt{A}$	1.50	2.02	$2.08 \pm 0.04$
Aschwanden et al. 2000 .....	Loop	1.44	$1.79 \pm 0.08$	$1.81 \pm 0.09$

the projected area and volume of avalanches are estimated from “instantaneous” snapshots of avalanches at their peak. Figure 3 shows a scatter plot of time-integrated projected area versus peak projected area, which is well fitted through a power law with index  $\delta = 1.35(\pm 0.01)$ , extending about 2 orders of

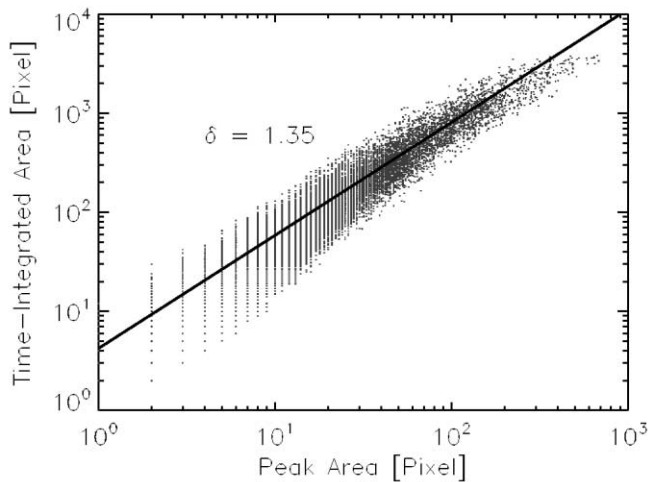


FIG. 3.—Scatter plot of the time-integrated and peak avalanche projected areas, both measured in “pixels” ( $\equiv$  lattice nodes) for the same  $64^3$  lattice simulation as shown in Fig. 2. A power law with index  $\delta = 1.35(\pm 0.01)$  yields a good fit. The slight downturn of data points at the upper right of the plot is due to the finite size of the lattice, as the projected area is clearly bounded above as  $A_{\max} = N^2 (= 4096)$  here.

magnitude in time-integrated area. This offers a potentially interesting observational test for the geometric properties of flares/avalanches, as observed with high spatial resolution and temporal cadence.<sup>2</sup> The exact value of the power-law index might be difficult to reliably infer, in view of unavoidable detection threshold effects. Moreover, observationally even an “instantaneous” snapshot involves some level of time integration. Nonetheless, the projected peak and time-integrated avalanche areas should definitely be related via a power law, with index significantly larger than unity. If not, then something is seriously amiss with the avalanche model for solar flares.

S. W. M. acknowledges the past support of the NCAR Advanced Study Program and is currently supported by an External Fellowship from the European Space Agency at GSFC. The National Center for Atmospheric Research is sponsored by the National Science Foundation.

<sup>2</sup> It is trivially obvious that the time-integrated area should be larger than the peak area; it is far less obvious that the two should be related via a power law, as they are here in the avalanche model. This power-law form is again a consequence of the spatial self-similarity of avalanches in the SOC state.

#### REFERENCES

- Aschwanden, M. J., Tarbell, T. D., Nightingale, R. W., Schrijver, C. J., Title, A., Kankelborg, C. C., Martens, P., & Warren, H. P. 2000, *ApJ*, 535, 1047  
 Bak, P., Tang, C., & Wiesenfeld, K. 1987, *Phys. Rev. Lett.*, 59, 381  
 Brown, J. C., Dwivedi, B. N., Sweet, P. A., & Almelady, Y. M. 1991, *A&A*, 249, 277  
 Charbonneau, P., McIntosh, S. W., Liu, H., & Bogdan, T. J. 2001, *Sol. Phys.*, 203, 321  
 Craig, I. J. D., & Brown, J. C. 1976, *A&A*, 49, 239  
 Dennis, B. 1985, *Sol. Phys.*, 100, 465  
 Jensen, H. J. 1998, *Self-Organized Criticality* (Cambridge: Cambridge Univ. Press)  
 Krucker, S., & Benz, A. O. 1998, *ApJ*, 501, L213  
 Lu, E. T. 1995, *ApJ*, 446, L109  
 Lu, E. T., & Hamilton, R. J. 1991, *ApJ*, 380, L89  
 Lu, E. T., Hamilton, R. J., McTiernan, J. M., & Bromund K. R. 1993, *ApJ*, 412, 841  
 McIntosh, S. W. 2000, *ApJ*, 533, 1043  
 McIntosh, S. W., Charbonneau, P., Bogdan, T. J., Liu, H., & Norman, J. P. 2001, *Phys. Rev. E.*, submitted  
 Mitra-Kraev, U., & Benz, A. O. 2001, *A&A*, 373, 318  
 Raymond, J. C., & Doyle, J. G. 1981, *ApJ*, 247, 686  
 Parker, E. N. 1988, *ApJ*, 330, 474  
 Parnell, C. E., & Jupp, P. E. 2000, *ApJ*, 529, 554